

Study on cutting force and surface micro-topography of hard turning of GCr15 steel

Tao Chen · Suyan Li · Bangxin Han · Guangjun Liu

Received: 13 October 2013 / Accepted: 10 March 2014 / Published online: 28 March 2014
© Springer-Verlag London 2014

Abstract This work investigates the cutting force and surface micro-topography in hard turning of GCr15 bearing steel. A series of experiments on hard turning of GCr15 steel with polycrystalline cubic boron nitride (PCBN) tools are performed on a CNC machining center. Experimental measurements of cutting force, 3D surface micro-topography, and surface roughness of the workpiece are performed. The 3D surface micro-topography of the workpiece is discussed, and the formation mechanism of the 3D surface is analyzed. The influence of cutting speed and feed rate on cutting force and surface roughness are discussed. The 2D and 3D surface roughness parameters are compared and discussed. It is found that feed rate has greater influence on cutting force and surface roughness than cutting speed and there exists the most appropriate cutting speed under which the minimum surface roughness can be generated while a relatively small cutting force can be found. Recommendations on selecting cutting parameters of hard turning of GCr15 steel are also proposed.

Keywords Hard turning · GCr15 steel · Cutting force · Surface micro-topography · Surface roughness

1 Introduction

Hardened steel is extensively used in industries to manufacture bearings, gears, shafts, and cams requiring tight geometric tolerances, longer service life, and good surface roughness [1]. Generally, hardened steel is finished in its hardened state by

grinding process to achieve surface integrity [2]. However, the grinding process of hardened steel has the disadvantages of low efficiency and time consuming. Therefore, hard turning which employs a single-point cutting tool and high speeds to machine ferrous alloys has become an attractive alternative to grinding process [3]. Hard turning provides surface roughness, dimensional and shape tolerances similar to those achieved in grinding, and has the advantage of cutting complex geometries, elimination of coolant, higher metal removal rates, and greater flexibility with a single machine setup when compared with the grinding process [4, 5].

Polycrystalline cubic boron nitride (PCBN) tool is the most widely used turning inserts for finish hard turning of hardened steels because of its high hardness, wear resistance, and thermal stability [6]. PCBN tool is more economical and cost-effective than ceramic tool and cemented carbide tool for a wide range of roughing and finishing applications. Hard turning with PCBN tool can achieve surface roughness which is equal to or even better than that by grinding [7].

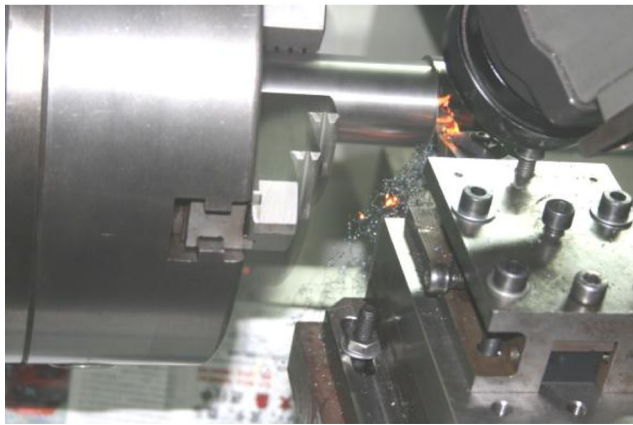
Hard turning with PCBN tool usually involves high cutting force, high temperature, and sawtooth chips, which will finally affect the machining quality. PCBN tool is usually chamfered to enhance the strength of the cutting edge and avoid early failure [8]. However, the chamfer also makes an increase in cutting force, and the cutting tool is subjected to cutting forces that are concentrated over a relatively small contact area on the rake face and the flank [9]. Hard turning is characterized by a high temperature due to dry machining of difficult-to-cut materials. The cutting mechanisms of hardened steel lead to the formation of sawtooth chips which are periodic and formed of identical segments [10, 11]. Those above-mentioned aspects will finally influence the cutting process and surface integrity. The surface topography produced by hard turning differs from that produced by grinding. Hard turning will naturally produce a more anisotropic surface [12]. The study of surface topography is very essential as it directly impacts the component

T. Chen · S. Li
School of Mechanical and Power Engineering, Harbin University of Science and Technology, Harbin 150080, People's Republic of China

B. Han · G. Liu (✉)
School of Mechanical Engineering, Tongji University,
Shanghai 200092, People's Republic of China
e-mail: gjliu@126.com



(a) The experimental set-up after clamping



(b) The hard turning experiment of GCr15 steel

Fig. 1 Experimental setup. **a** The experimental setup after clamping. **b** The hard turning experiment of GCr15 steel

functionality, such as friction, wear, and fatigue. The bulk surface profile data in hard turning is mostly limited to 2D line tracing which may not be efficient in characterizing the surface [13], and there is a need to study the 3D surface generated by hard turning. Despite the advantages of PCBN tool and extensive studies on hard turning [14–16], there is a clear need for

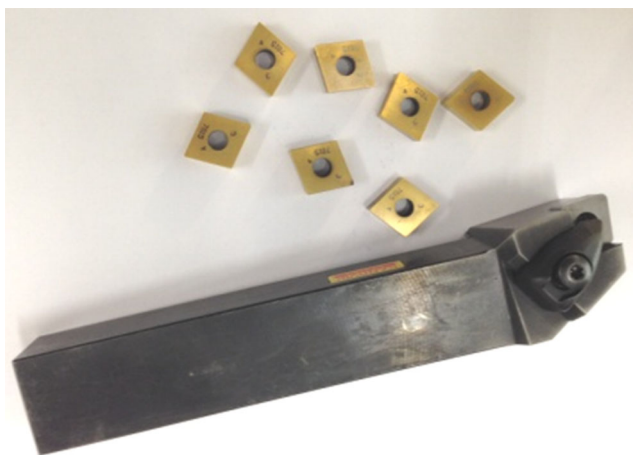


Fig. 2 The PCBN tools

Table 1 Geometric parameters of the PCBN tools

Parameter	Value
Rake angle (°)	0
Clearance angle (°)	7
inclination angle (°)	0
cutting edge angle (°)	95
Chamfer angle (°)	−30
Chamfer width (mm)	0.1
Corner radius (mm)	0.4

further research to clarify the issues in the areas of cutting force, cutting temperature, surface topography, etc.

In this work, a series of experiments of hard turning of GCr15 bearing steel using PCBN tools are conducted. Cutting force, 3D surface micro-topography, and surface roughness are measured. The variations of cutting force and surface roughness parameters with cutting parameters are investigated. The characteristics of the turned 3D surface micro-topography are analyzed and discussed.

2 Experimental procedure

Experiments on cylindrical turning of bearing outer rings are conducted on the CNC machining center PUMA 230MSB. Experimental setup after clamping is shown in Fig. 1a, and the experiment system in hard turning is shown in Fig. 1b. Eight coated Sandvik CNGA120404S01030A 7015 PCBN tools, as shown in Fig. 2, are employed in the experiments, and each set of cutting parameters uses one tool. The geometric parameters of the PCBN tools are listed in Table 1. Experimental conditions are shown in Table 2. No cutting fluids or coolants are used.

The workpiece shown in Fig. 3 is a bearing outer ring with a 47-mm diameter and 14-mm width, and its material is GCr15 hardened bearing steel with the hardness of 60 HRC. The chemical composition of GCr15 steel is listed in Table 3.

The cutting forces during turning operations are measured by using a three-component dynamometer (Kistler 9257BA), a multi-channel charge amplifier (Kistler 5019B), a data

Table 2 Experimental conditions

Experiment number	Cutting speed v_c (m/min)	Feed rate f (mm/r)	Axial depth of cut a_p (mm)
1	100	0.05	0.1
2	150		
3	200		
4	300		
5	100	0.1	
6	150		
7	100	0.15	
8	150		



Fig. 3 The GCr15 steel workpiece

acquisition card (PCI-8335A), and a computer data acquisition software (DynoWare3 System). The forces recorded are the main cutting force, feed force, and radial force. The dynamometer is mounted on the machining center, and the tool holder is mounted on the top of the dynamometer.

The 3D surface micro-topography and 3D surface roughness Sa of the workpiece are examined by using the confocal laser scanning microscopy Zeiss Axio CSM 700. The 2D surface roughness Ra for each cutting condition is measured by using a roughness meter.

3 Results and discussion

3.1 Cutting force

Figure 4 shows the variation of cutting force with cutting speed. The cutting force decreases when increasing cutting speed from 100 to 200 m/min, as the cutting temperature increases with cutting speed and high cutting temperature has a softening effect to the workpiece material. However, the cutting force increases when increasing cutting speed from 200 to 300 m/min, as the cutting temperature gradually increases and is close to the melting point of the workpiece material, then effects of the cutting temperature on the cutting force is weakened. It is well known a large number of heat is generated in hard turning. The heat resistance of PCBN tool can be 1,000–1,500 °C, and PCBN has a high hardness in high temperature. Therefore, it is beneficial to take advantage of the

Table 3 Chemical composition of GCr15 steel (mass%)

C	Mn	Si	Cr	S	P	Fe
0.95–1.05	0.20–0.40	0.15–0.35	1.30–1.65	<0.020	<0.027	Balance

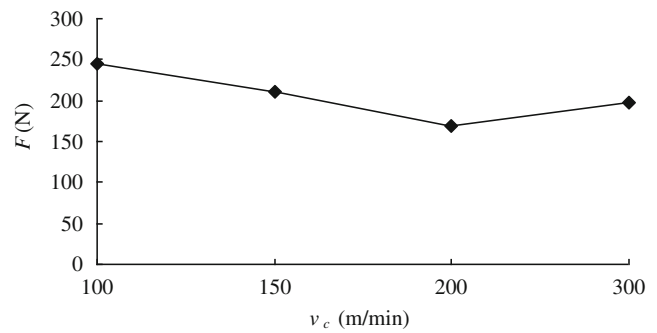
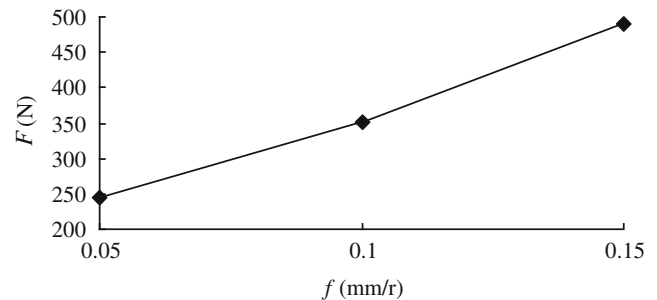


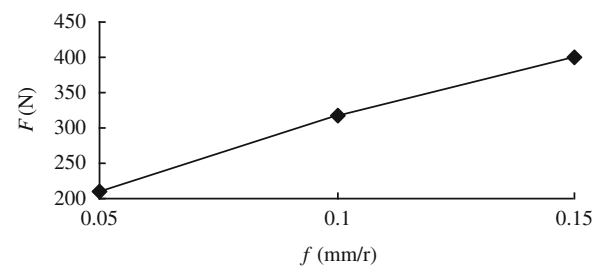
Fig. 4 Cutting speed versus cutting force ($f=0.05$ mm/r, $a_p=0.1$ mm)

hardness difference between PCBN and GCr15 steel to improve cutting efficiency and tool life.

Figure 5 shows the variation of cutting force with feed rate. It is seen that the cutting forces increase with increasing feed rate. Compared with Fig. 4, feed rate has a greater influence on the cutting force than cutting speed. This can be explained by increasing chip cross section with increasing feed rate [17, 18]. With the increasing of feed rate, the material removal rate and plastic deformation rate are increased, resulting in an increasing of the cutting force. PCBN tools are generally used for finish machining, and axial depth of cut is usually small. Therefore, a relative large feed rate is recommended to produce a metal-softening effect. It should be noted that feed rate has a greater influence on cutting force than cutting speed. Doubling the feed rate results in about 1.5 times of the cutting force and makes the actual chip twice as thick thus making it much more difficult to curl and bend.



(a) $v_c=100$ m/min, $a_p=0.1$ mm



(b) $v_c=150$ m/min, $a_p=0.1$ mm

Fig. 5 Feed rate versus cutting force. **a** $v_c=100$ m/min, $a_p=0.1$ mm. **b** $v_c=150$ m/min, $a_p=0.1$ mm

3.2 Surface roughness

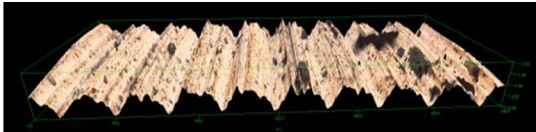
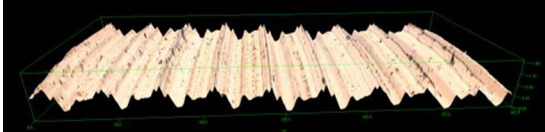
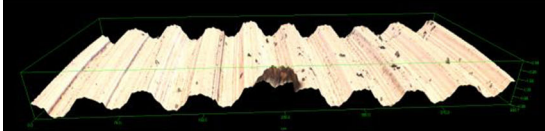
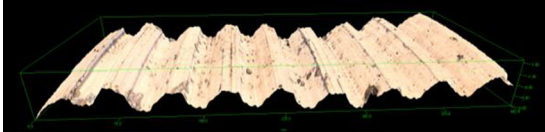
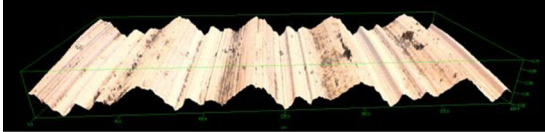
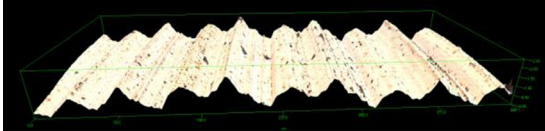
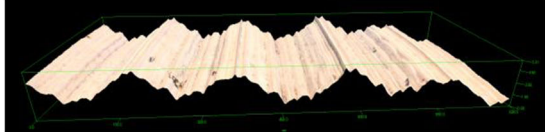
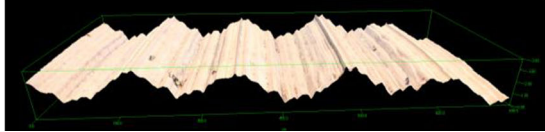
3.2.1 3D surface micro-topography

In turning, the tool has a spiral motion relative to the workpiece and a linear feeding motion along the axial direction of the workpiece. Therefore, the machined surface is not a smooth cylindrical one but a remaining one between two

adjacent tool profiles. The surface roughness caused by geometry is known as theoretical roughness. However, the surface roughness generated by machining may be more different than theoretical roughness, as the surface roughness is influenced by lots of factors, such as tool geometries, cutting parameters, tool wear, machine tools, etc.

The 3D surface micro-topography of the workpiece of each experiment program is shown in Table 4. Compared with

Table 4 3D surface micro-topography

Experiment number	3D surface micro-topography	Maximum height (μm)
1		2.00
2		1.80
3		2.50
4		1.80
5		3.79
6		2.43
7		5.51
8		3.85

grinding [19], a single cutting edge with defined geometry is used in hard turning to generate the machined surface, which generates a better surface integrity. The feed rate and geometry parameters of the tool determine the symmetrical topography of the machined surface [13]. The 3D surface along the axial direction of the machined workpiece is a contour shape with well-defined peaks and valleys, and the spacing between two peaks is the value of feed rate (mm/r). As the majority of generated heat in hard turning is carried away by the chips, thermal damage of the machined surface is rarely seen and hard turning is more easily to keep surface integrity of the workpiece. In the experiments, hard turning produces a better surface than grinding [19]. It has been demonstrated that hard turning can produce an as-good or even better surface than grinding [20, 21]. The 3D surface micro-topography images allow distinguishing mixed anisotropic textures in machining.

Table 4 shows that increasing feed rate results in the increasing of surface roughness when comparing experiment nos. 1, 5, and 7. However, a too-low feed rate will not generate a desired surface roughness. As only tool tip involves in machining in hard turning, if the feed rate is too low, the tool corner radius will “crawl” on the workpiece surface, which is not a normal cutting state.

3.2.2 2D Surface roughness

Figure 6 shows the variation of 2D surface roughness Ra with cutting speed. It is seen that the surface roughness decreases with the increasing of cutting speed first, as the increasing of cutting speed generates high cutting temperature which causes metal softening effects and reduces cutting force. Therefore, the surface roughness decreases.

When the cutting speed reaches 200 m/min, the surface roughness increases, as the cutting temperature increases with cutting speed, and the tool wear is increased with the increasing of cutting temperature, which results in an increase in the friction between the tool, chip, and workpiece. Sawtooth chips are formatted when the cutting speed is 200 m/min. Sawtooth chip formation can be characterized as a periodic process, which results in the cutting force oscillations and vibrations of the tool system and ultimately affects the machined surface integrity [21–23]. Furthermore, built up edge (BUE) is more

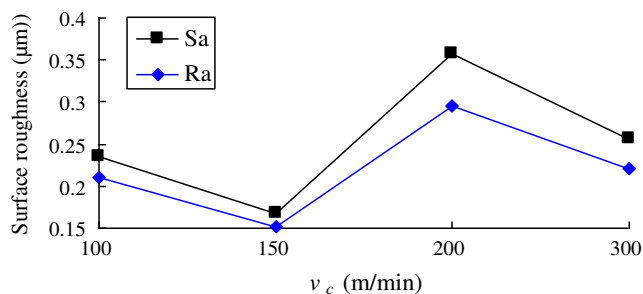


Fig. 6 Cutting speed versus surface roughness ($f=0.05$ mm/r, $a_p=0.1$ mm)

easily to be generated at moderate cutting speed 200 m/min. Therefore, it is recommended to avoid the critical speed that generated sawtooth chip and BUE to improve production efficiency while ensuring machining quality.

When the cutting speed reaches 300 m/min, the surface roughness decreases. With the increasing of cutting speed, the heat transfers to the chips increases, and the heat taken away by the chips also increases. Meanwhile, the heat transfers to the tool, the workpiece decreases, and there is no enough time to heat the tool and workpiece, which causes a decrease in cutting temperature. Therefore, the tool can be in a good cutting state and the surface roughness will decrease.

The variation of 2D surface roughness Ra with feed rate is shown in Fig. 7. The surface roughness increases with the increasing of feed rate, as increasing feed rate results in increasing chip cross section. With the increase in feed rate, the material removal rate and plastic deformation rate are increased, resulting in the increase in the cutting forces and cutting vibration, and finally a decrease in surface roughness is found. Compared with Fig. 6, it is seen that feed rate has greater influence on the surface roughness than cutting speed, and feed rate less than 0.1 mm/r is recommended.

3.2.3 3D Surface roughness

It is already known that Ra cannot give detailed information of the machined surface, as the profile is only a small area of the machined surface. The arithmetic mean deviation Sa is introduced to characterize the 3D surface in this work. The

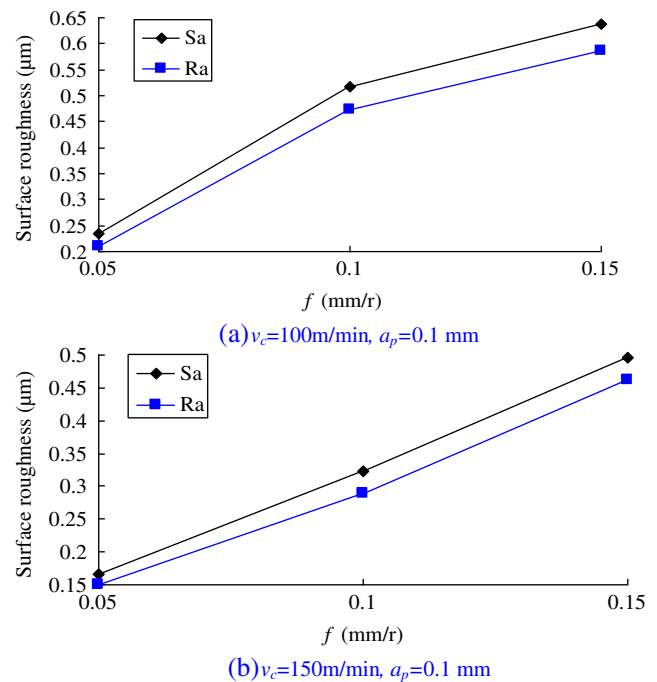


Fig. 7 Feed rate versus surface roughness. a $v_c=100$ m/min, $a_p=0.1$ mm. b $v_c=150$ m/min, $a_p=0.1$ mm

arithmetic mean deviation S_a is expanded from R_a and expresses the arithmetic mean of the absolute surface asperity departures from the reference datum within the sampling area.

Figure 6 also shows the variation of 3D surface roughness S_a with cutting speed. Figure 7 shows the variation of S_a with feed rate. It is seen that the 3D surface roughness S_a shows similar trends with the 2D surface roughness R_a . According to the definition of S_a , it can characterize much more surface characteristics and therefore may better represent a surface as a whole [13]. In 3D arrangements, the characteristics of the machined surface can be better distinguished than in 2D arrangements [24].

4 Conclusions

1. An experiment setup on measuring cutting forces, 3D surface micro-topography, and surface roughness R_a and S_a in hard turning of GCr15 steel is proposed. The effects of cutting parameters on cutting force and surface roughness is discussed. The 3D surface micro-topography generated by hard turning is analyzed.
2. Feed rate has more significant influence on cutting force and surface roughness than cutting speed. The cutting force and surface roughness both increase with increasing feed rate. There exists the most appropriate cutting speed under which the minimum surface roughness can be generated while a relatively small cutting force can be found.
3. The 3D surface roughness S_a shows similar trends with the 2D surface roughness R_a . As 3D surface roughness parameters can reflect more surface characteristics, it is recommend adopting both 2D and 3D surface roughness parameters to evaluate the machining quality.
4. The 3D surface micro-topography reflects the cutting parameters and geometries of the cutting edge. The 3D surface along the axial direction of the workpiece is a contour shape with well-defined peaks and valleys, and the spacing between two peaks is the value of feed rate (mm/r). Thermal damage of the machined surface is rarely seen, and hard turning is more easily to keep surface integrity of the workpiece.

Acknowledgments The authors would like to acknowledge the support of the National Natural Science Foundation of China under Grant No. 51005064, the Natural Science Foundation of Heilongjiang Province under Grant No. QC2011C129, the Opening Foundation of Key Laboratory of Advanced Manufacturing Technology and Tool Development of Universities in Heilongjiang Province, the Fundamental Research Funds for the Central Universities, the Program for Harbin Science & Technology Innovation Talents under Grant No. 2012RFQXG078, and the Distinguished Young Talents Program of Harbin University of Science and Technology.

References

1. Rashid WB, Goel S, Luo X, Ritchie JM (2013) An experimental investigation for the improvement of attainable surface roughness during hard turning process. *Proc Inst Mech Eng B J Eng Manuf* 227: 338–342
2. Jouini N, Revel P, Mazeran PE, Bigerelle M (2013) The ability of precision hard turning to increase rolling contact fatigue life. *Tribol Int* 59:141–146
3. Ding H, Shin YC (2013) Multi-physics modeling and simulations of surface microstructure alteration in hard turning. *J Mater Process Technol* 213:877–886
4. Oliveir AJ, Diniz AE, Ursolino DJ (2009) Hard turning in continuous and interrupted cut with PCBN and whisker-reinforced cutting tools. *J Mater Process Technol* 209:5262–5270
5. Aouici H, Yallese MA, Chaoui K, Mabrouki T, Rigal J (2011) Analysis of surface roughness and cutting force components in hard turning with CBN tool: prediction model and cutting conditions optimization. *Measurement* 45:344–353
6. Dureja JS, Gupta VK, Sharma VS, Dogra M (2010) Wear mechanisms of coated mixed-ceramic tools during finish hard turning of hot tool die steel. *Proc Inst Mech Eng C J Mech Eng Sci* 224: 183–193
7. Guddat J, M'Saoubi R, Alm P, Meyer D (2011) Hard turning of AISI 52100 using PCBN wiper geometry inserts and the resulting surface integrity. *Procedia Eng* 19:118–124
8. Choudhury IA, See NL, Zuhairi M (2005) Machining with chamfered tools. *J Mater Process Technol* 170:115–120
9. Singh D, Rao PV (2010) Flank wear prediction of ceramic tools in hard turning. *Int J Adv Manuf Technol* 50:479–493
10. Poulachon G, Al M (2000) Hard turning: chip formation mechanisms and metallurgical aspects. *J Manuf Sci Eng* 122:406–412
11. Barry J, Byrne G (2002) The mechanisms of chip formation in machining hardened steels. *J Manuf Sci Eng* 124:528–535
12. Elbah M, Yallese MA, Aouici H, Mabrouki T, Rigal JF (2013) Comparative assessment of surface roughness produced by hard machining with mixed ceramic tools including 2D and 3D analysis. *Measurement* 46:3041–3056
13. Waikar RA, Guo YB (2007) A comprehensive characterization of 3D surface topography induced by hard turning versus grinding. *J Mater Process Technol* 197:189–199
14. Jafarian F, Amirabadi H, Sadri J (2013) Integration of finite element simulation and intelligent methods for evaluation of thermo-mechanical loads during hard turning process. *Proc Inst Mech Eng B J Eng Manuf* 227:235–248
15. Hessainia Z, Belbah A, Yallese MA, Mabrouki T, Rigal JF (2013) On the prediction of surface roughness in the hard turning based on cutting parameters and tool vibrations. *Measurement* 46:1671–1681
16. Sadik MI (2012) Wear development and cutting forces on CBN cutting tool in hard part turning of different hardened steels. *Procedia CIRP* 1:232–237
17. Korkut I, Donertas MA (2007) The influence of feed rate and cutting speed on the cutting forces, surface roughness and tool-chip contact length during face milling. *Mater Des* 28:308–312
18. Kumar KVBSK, Choudhury SK (2008) Investigation of tool wear and cutting force in cryogenic machining using design of experiments. *J Mater Process Technol* 203:95–101
19. Yue C, Liu X, Wang Y, Hu J (2008) Surface integrity of hard cutting and grinding processes. *Tool Engineering* 42:13–18
20. Matsumoto Y, Hashimoto F, Lahoti G (1999) Surface integrity generated by precision hard turning. *CIRP Ann Manuf Technol* 48: 59–62

21. Zhang X, Liu CR, Wu S, Wang H (2011) Predicting the effects of cutting parameters and tool geometry on hard turning process using finite element method. *J Manuf Sci Eng* 133:041010-1–13
22. Dogra M, Sharma VS, Sachdeva A, Suri NM, Dureja JS (2011) Performance evaluation of CBN, coated carbide, cryogenically treated uncoated/coated carbide inserts in finish-turning of hardened steel. *Int J Adv Manuf Technol* 57:541–553
23. Bushlya V, Zhou J, Avdovic P, Stahl J (2011) Performance and wear mechanisms of whisker-reinforced alumina, coated and uncoated PCBN tools when high-speed turning aged Inconel 718. *Int J Adv Manuf Technol* 66:2013–2021
24. Zawada-Tomkiewicz A (2011) Analysis of surface roughness parameters achieved by hard turning with the use of PCBN tools. *Estonian J Eng* 17:88–99